ISSN (E): 2181-4570 ResearchBib Impact Factor:6,4 / 2023 SJIF 2024 = 5.073/Volume-2, Issue-10

Describing Lorentz transformations, Doppler's effect, Hubble's law, and others in curvilinear coordinates using generalized biquaternions

Babaev A. Kh.

PhD of Phys. & Math Sciences, National University (Rep. Uzb), NSTU (RF) (former), Freelancer, e-mail: prepadamira@gmail.com

Abstract.

The paper presents the derivation of Lorentz transformations in curvilinear coordinates using a generalized biquaternions method. The orbital rotation of the source and/or receiver, i.e. (mathematically) the Lorentz transformation in spherical coordinates, is the cause of the transverse Doppler effect. The change of the wave frequency, i.e., «redshift" leads to nonlinearities of Hubble's law, e.g., accelerated and anisotropic expansion of the Universe, aberration, and wave polarization.

Keywords:

Biquaternion; Lorentz transformation in spherical coordinates; "redshift"; nonlinearity of the Hubble's law; accelerated expansion of the universe; aberration and polarization of starlight.

UDC 524.8: 512.7

Introduction

The cause of the wave frequency shift is the satellite's orbital motion, i.e., the transverse motion of the signal source in a direction perpendicular to the observer. This is the transverse Doppler effect [1]. The signal frequency offset (redshift) is a function of the orbital altitude and velocity of the satellite: $\Delta\omega = f(h, v)$. Corrections [2] to adjust the data are always introduced into the calculations in satellite navigation.

ISSN (E): 2181-4570 ResearchBib Impact Factor:6,4 / 2023 SJIF 2024 = 5.073/Volume-2, Issue-10

The classical form of the transverse Doppler effect (in the Cartesian coordinate system) is a strong simplification that limits the generalization of this law to describe many phenomena.

The purpose of this paper is to find the Lorentz transformation [3] and its consequences, the Doppler effect and aberration, in general form in curvilinear coordinates. This approach is universal and applicable to understand better the mechanisms of phenomena such as the accelerated [4] and anisotropic [5] expansion of the Universe, as well as the nonlinear nature of the Hubble law and parameter [6].

Results

Theoretical basis.

1. Biquaternions in Cartesian coordinates

In abstract (Clifford) algebra, rotations (transformations) on planes in pseudo-Euclidean space are given by formulas:

$$x' = R_\alpha x \tilde{R}_\alpha \qquad (1)$$

or

$$x = \tilde{R}_\alpha x' R_\alpha \qquad (2)$$

Here

R_α is biquaternion, $\tilde{R}_\alpha$ is inverse or complex-conjugate biquaternion [7]:

$$R_\alpha(\tilde{R}_\alpha) = exp(\pm\gamma_\alpha\gamma_0\frac{z_\alpha}{2}) = I\,cosh\frac{I\eta_\alpha+\gamma\varphi_\alpha}{2} \pm \gamma_\alpha\gamma_0\,sinh\frac{I\eta_\alpha+\gamma\varphi_\alpha}{2} \qquad (3)$$

I is a unit 4x4 matrix;

ISSN (E): 2181-4570 ResearchBib Impact Factor:6,4 / 2023 SJIF 2024 = 5.073/Volume-2, Issue-10

$x = \sum_{i=0}^{3} \gamma_i \cdot x^i$ is space-time vector in the stationary coordinate system (K);

$x' = \sum_{i=0}^{3} \gamma_i \cdot x'^i$ is the same vector in the moving coordinate system (K');

γ_0, γ_α, $\alpha = 1,2,3$ are Dirac matrices;

$\gamma = \gamma_0\gamma_1\gamma_2\gamma_3$ is a matrix analog of imaginary unit ($\gamma^2 = -I$);

$\gamma_\alpha\gamma_0 \frac{z_\alpha}{2}$ is a bivector;

$z_\alpha = I\eta_\alpha + \gamma\varphi_\alpha$ is a complex matrix.

φ_α are "purely spatial" rotations on the *x0y*, *y0z*, *z0x* planes. Since we will only consider Lorentz transformations, we will omit these rotations in the following.

η_α are angles of rotation of the *t0x*, *t0y*, *t0z* planes, or so-called rapidities.

It is obvious that

$$R_\alpha {R_\alpha}^{-1} = R_\alpha \tilde{R}_\alpha = I \qquad (4)$$

The algorithm ((1) and/or (2)) is explained in various sources, such as [8].

<u>*Note*</u>. If there is no sum sign ($\sum_\alpha x_\alpha$), then there is no summation, i.e., no summation over repeated indices (Einstein's convention). For example, there is no summation over α in $R_\alpha \tilde{R}_\alpha$ or $g_{\alpha\alpha}k^\alpha x^\alpha$.

2. <u>*Biquaternions in generalized form*</u>

The generalization of the transformations (1) and (2) in curvilinear coordinates will be the following formulas:

$$x' = \mathcal{R}_\alpha x \tilde{\mathcal{R}}_\alpha \qquad (5)$$

ISSN (E): 2181-4570 ResearchBib Impact Factor:6,4 / 2023 SJIF 2024 = 5.073/Volume-2, Issue-10

or $$x = \tilde{\mathcal{R}}_\alpha x' \mathcal{R}_\alpha \qquad (6)$$

Here $\mathcal{R}_\alpha$ and $\tilde{\mathcal{R}}_\alpha$ are a biquaternion and an inverse biquaternion in a generalized form [9]:

$$\mathcal{R}_\alpha(\tilde{\mathcal{R}}_\alpha) = \frac{1}{|\tau_{\alpha 0}|}\left(I|\tau_{\alpha 0}|\, cosh\frac{z_\alpha}{2} \pm \tau_{\alpha 0}\, sinh\frac{z_\alpha}{2}\right) \qquad (7)$$

$x = \sum_{i=0}^{3} e_i\, x^i$ is a 4-vector in a fixed basis K;

$x' = \sum_{i=0}^{3} e_i\, x^{i'}$ is the same vector in the moving basis K';

$\tau_{\alpha 0} = e_\alpha \Lambda e_0$ is the bivector, i.e. the outer product of vectors e_α and e_0 [10].

$|\tau_{\alpha 0}| = |e_\alpha \Lambda e_0| = I\sqrt{g_{\alpha 0} g_{\alpha 0} - g_{00} g_{\alpha\alpha}}$ is the modulus ("length") of the bivector $e_\alpha \Lambda e_0$ [11].

g_{ij} is a matric tensor.

e_ι are vectors in the system of curvilinear coordinates.

The set of four such vectors $\{e_\iota\}$ forms a local basis (frame) in the 4-dimensional space.

Λ and • are symbols of outer and inner products of vectors [10].

It is obvious that the biquaternions (7) satisfy the condition:

$$\mathcal{R}_\alpha \bullet \tilde{\mathcal{R}}_\alpha = I$$

Note. The name "vector" for e_ι is conventional. In reality, e_ι are 4x4 matrices related to Dirac matrices through coordinate transformation functions $X_i(q^j)$:

$$e_i = \sum_{j=0}^{3} \frac{\partial X_j}{\partial q^i} \gamma_j$$

3. Lorentz transformation in generalized form.

ISSN (E): 2181-4570 ResearchBib Impact Factor:6,4 / 2023 SJIF 2024 = 5.073/Volume-2, Issue-10

Let us find the explicit form of the transformation (6). Let us substitute the biquaternions (7), x' and x into (6).

By Clifford's double cross product [11]

$$z \bullet (x \wedge y) = -(x \wedge y) \bullet z = (z \bullet x)y - (z \bullet y)x \qquad \textbf{(8)},$$

we can write

$$x = \tilde{\mathcal{R}}_\alpha \bullet x' \bullet \mathcal{R}_\alpha = \tilde{\mathcal{R}}_\alpha \bullet \tilde{\mathcal{R}}_\alpha \bullet x' \qquad \textbf{(9)}$$

Indeed, the identity

$x' \bullet \mathcal{R}_\alpha = \tilde{\mathcal{R}}_\alpha \bullet x'$,

takes place, since vectors $e_0 x'^0$ and $e_\alpha x'^\alpha$ commutate with $I|(e_\alpha \wedge e_0)|\, cosh\frac{z_\alpha}{2}$, but anticommutate with $(e_\alpha \wedge e_0)\, sinh\frac{z_\alpha}{2}$.

In curvilinear coordinates, the products of $e_0 \bullet \tau_{\alpha 0}$ and $e_\alpha \bullet \tau_{\alpha 0}$ are [12]:

$$e_0 \bullet \tau_{\alpha 0} = -\tau_{\alpha 0} \bullet e_0 = e_0 \bullet (e_\alpha \wedge e_0) = (e_0 \bullet e_\alpha)e_0 - (e_0 \bullet e_0)e_\alpha = -g_{00}e_\alpha \qquad \textbf{(10.1)}$$

$$e_\alpha \bullet \tau_{\alpha 0} = -\tau_{\alpha 0} \bullet e_\alpha = e_\alpha \bullet (e_\alpha \wedge e_0) = (e_\alpha \bullet e_\alpha)e_0 - (e_\alpha \bullet e_0)e_\alpha = g_{\alpha\alpha}e_0 \qquad \textbf{(10.2)}$$

For simplicity, we will consider an orthogonal coordinate system, i.e.

$e_\iota \bullet e_j = g_{ii}$, if $i = j$ and $e_\iota \bullet e_j = 0$, if $i \neq j$.

Accordingly $|\tau_{\alpha 0}| = |e_\alpha \wedge e_0| = I\sqrt{-g_{00}g_{\alpha\alpha}}$.

Then from equation (9) we get

$$x = e_0 x^0 + e_\alpha x^\alpha = \frac{1}{\tau_{\alpha 0}^2}(I\tau_{\alpha 0}^2 cosh\eta_\alpha + |\tau_{\alpha 0}|\tau_{\alpha 0} sinh\eta_\alpha) \bullet (e_0 x'^0 + e_\alpha x'^\alpha)$$

ISSN (E): 2181-4570 ResearchBib Impact Factor:6,4 / 2023 SJIF 2024 = 5.073/Volume-2, Issue-10

We substitute (10.1) and (10.2) into this equality. Multiplying the brackets and simplifying, we get

$$x = \frac{e_0\tau_{\alpha 0}^2 cosh\eta_\alpha x'^0 + e_\alpha \tau_{\alpha 0}^2 cosh\eta_\alpha x'^\alpha + e_\alpha g_{00}|\tau_{\alpha 0}| sinh\eta_\alpha x'^0 - g_{\alpha\alpha} e_0 |\tau_{\alpha 0}| sinh\eta_\alpha x'^\alpha}{\tau_{\alpha 0}^2}$$

Separating this equality by vectors e_0 and e_α and simplifying, we get the Lorentz transformation in curvilinear coordinates:

$$\begin{cases} x^0 = cosh\eta_\alpha \cdot x'^0 + \frac{|\tau_{\alpha 0}|}{g_{00}} sinh\eta_\alpha \cdot x'^\alpha \\ x^\alpha = cosh\eta_\alpha \cdot x'^\alpha - \frac{|\tau_{\alpha 0}|}{g_{\alpha\alpha}} sinh\eta_\alpha \cdot x'^0 \end{cases} \qquad \textbf{(11)}$$

Formula (11) is the Lorentz transformation in generalized form.

4. <u>Generalized form of the Doppler effect and aberration.</u>

Now we can derive the Doppler effect in curvilinear coordinates from (11). The change of frequency and direction of propagation (aberration of light) of a spherical monochromatic wave are determined by the condition of equality of phases of the same wave in both frames of reference [13]:

$$g_{00}k'^0 x'^0 + g_{\alpha\alpha}k'^\alpha x'^\alpha = g_{00}k^0 x^0 + g_{\alpha\alpha}k^\alpha x^\alpha \qquad \textbf{(12)}$$

Substituting the values x^0, x^α from (11) into (12) and simplifying, we obtain:

$$g_{00}k'^0 x'^0 + g_{\alpha\alpha}k'^\alpha x'^\alpha =$$

$$= g_{00}k^0 cosh\eta_\alpha \cdot x'^0 - k^\alpha |\tau_{\alpha 0}| sinh\eta_\alpha \cdot x'^0 + k^0 |\tau_{\alpha 0}| sinh\eta_\alpha \cdot x'^\alpha + g_{\alpha\alpha}k^\alpha cosh\eta_\alpha \cdot x'^\alpha$$

By comparing the coefficients of the same variables, we have:

ISSN (E): 2181-4570 ResearchBib Impact Factor:6,4 / 2023 SJIF 2024 = 5.073/Volume-2, Issue-10

$$k'^0 = k^0 cosh\eta_\alpha - \frac{|\tau_{\alpha 0}|}{g_{00}} k^\alpha sinh\eta_\alpha \qquad \textbf{(13.1)}$$

$$k'^\alpha = k^\alpha cosh\eta_\alpha + \frac{|\tau_{\alpha 0}|}{g_{\alpha\alpha}} k^0 sinh\eta_\alpha \qquad \textbf{(13.2)}$$

Formula (13.1) is the Doppler effect, and (13.2) is the aberration of the wave.

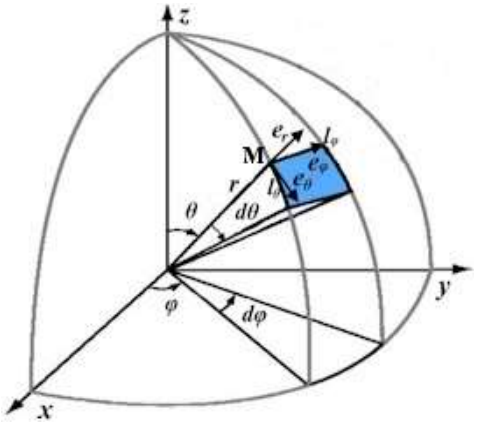

Figure 1.

<u>Note</u>. We will find the geometrical and physical meaning of the functions $cosh\eta_\alpha$, $sinh\eta_\alpha$, and $tanh\eta_\alpha$ in (11) and (13) (Fig. 1) in the spherical coordinate system.

The plane $e_\varphi M e_\theta$ touches the surface $l l_\varphi M l_\theta$ at the point M. For small angles $d\theta$ and $d\varphi$, the arcs $l_\varphi = r \cdot sin\theta \cdot d\varphi$ and $l_\theta = r \cdot d\theta$ are a little different from straight lines. As we are considering an orthogonal coordinate system, all axes (including the time axis) are perpendicular to each other. Therefore, we take the rotation in the plane tl_θ as in the classical case (in pseudo-Euclidean space):

$$cosh\eta_\theta = \frac{1}{\sqrt{1-\beta_\theta^2}}, \qquad sinh\eta_\theta = \frac{\beta_\theta}{\sqrt{1-\beta_\theta^2}}, \qquad tanh\eta_\theta = \beta_\theta, \qquad \beta_\theta = v_\theta/c.$$

v_θ is the linear velocity of system K' relative to system K in the direction of tangent vector e_θ. c is light velocity.

Also $cosh\eta_\varphi = \frac{1}{\sqrt{1-\beta_\varphi^2}}$, $sinh\eta_\varphi = \frac{\beta_\varphi}{\sqrt{1-\beta_\varphi^2}}$, $tanh\eta_\varphi = \beta_\varphi$, $\beta_\varphi = \frac{v_\varphi}{c}$.

v_φ is the linear velocity of the system K' relative to the system K in the direction of the tangent vector e_φ.

ISSN (E): 2181-4570 ResearchBib Impact Factor:6,4 / 2023 SJIF 2024 = 5.073/Volume-2, Issue-10

Since r is a straight line segment, the rotation in the plane $t0r$ does not differ from the classical case: $coshn\eta_r = 1/\sqrt{1-\beta_r^2}$, $sinhn\eta_r = \beta_r/\sqrt{1-\beta_r^2}$, $\beta_r = v_r/c$, v_r is the velocity along r.

Calculations

We will not give Lorentz transformations and wave aberrations in Cartesian coordinates. The reference of rotations on the $t0x$, $t0y$, $t0z$ planes in Minkowski space where $g_{00} = 1$, $g_{11} = g_{22} = g_{33} = -1$ and $|\tau_{\alpha 0}| = \sqrt{-g_{00}g_{\alpha\alpha}} = 1$ can be found in [13].

5. *Lorentz Transformations and the Doppler Effect in the Time-Spherical Coordinate System:* ct, r, θ, φ. (Figure 2.)

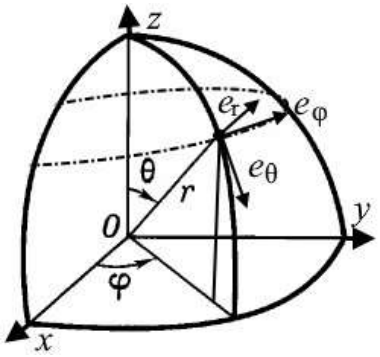

Let us find the form of the Lorentz transformation (11) and the Doppler effect (13.1) in the time-spherical coordinate system: $q^0 = ct$ is time or zero axis; $q^1 = r$ is the radius vector; $q^2 = \theta$ is zenith or polar angle; $q^3 = \varphi$ is the azimuthal angle. $0 \le t < \infty$, $0 \le r < \infty$, $0 \le \theta \le \pi$, $0 \le \varphi \le 2\pi$

Figure 2.

A) Let $\alpha = 3$, т.е. $x'^0 = ct'$, $x'^3 = \varphi'$, $x^0 = ct$, $x^3 = \varphi$, $g_{00} = 1$, $g_{33} = -r^2 \cdot sin^2\theta$, $|\tau_{30}| = r \cdot sin\theta$.

Then, from (11), we obtain the Lorentz transformations for the motion in the azimuthal plane with the velocity β_φ.

ISSN (E): 2181-4570 ResearchBib Impact Factor:6,4 / 2023 SJIF 2024 = 5.073/Volume-2, Issue-10

$$\begin{cases} ct = \frac{1}{\sqrt{1-\beta_\varphi^2}} \cdot (ct' + r \cdot sin\theta \cdot \beta_\varphi \cdot \varphi') \\ \varphi = \frac{1}{\sqrt{1-\beta_\varphi^2}} \cdot (\varphi' + \frac{\beta_\varphi}{r \cdot sin\theta} \cdot ct') \end{cases} \quad \textbf{(14)}$$

Let's find the type of Doppler effect and aberration. Our first objective is to determine the wave vector type for azimuthal motion β_φ ($\beta_r = 0,\ \beta_\theta = 0$) (Figure 3).

β_φ – velocity of system K' relative to K is tangent to the arc (along φ).

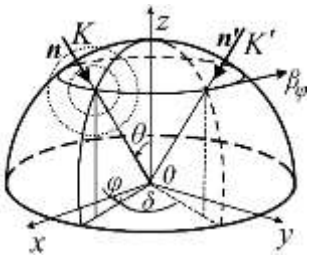

Figure 3.

The wave vector $\boldsymbol{n}$ is perpendicular to the front of a spherical monochromatic wave. The angle between $\boldsymbol{n}$ and x is equal to φ. The angle between vector $\boldsymbol{n}'$ and x is equal to x. The aberration angle δ is the angle between the vectors $\boldsymbol{n}$ and $\boldsymbol{n}'$.

From equation (13) we get

$$\omega' = \frac{\omega}{\sqrt{1-\beta_\varphi^2}} \cdot (1 - r \cdot sin\theta \cdot \beta_\varphi) \quad \textbf{(15.1)}$$

$$\omega' \cdot cos\delta = \frac{\omega}{\sqrt{1-\beta_\varphi^2}} \cdot (1 - \frac{\beta_\varphi}{r \cdot sin\theta}) \quad \textbf{(15.2)}$$

The aberration angle δ is the difference between the angle of wave incidence from the source and the observed angle, which varies due to the rotation of the receiver (e.g., the Earth) in orbit.

(15.1) is the Lorentz transformation and (15.2) is the aberration of the wave at the azimuthal velocity of the source (receiver). The aberration angle δ is defined relative to the wave vector $\boldsymbol{n}$ in formula (15.2).

We find δ relative to the observer (point 0) (Figure 3).

ISSN (E): 2181-4570 ResearchBib Impact Factor:6,4 / 2023 SJIF 2024 = 5.073/Volume-2, Issue-10

Since $\angle z\hat{}\,\boldsymbol{n} = \varphi$ and $\angle z\hat{}\,\boldsymbol{n}' = \varphi + \delta$, then

$$k^3 = \frac{\omega}{c}\cdot cos\varphi, \quad k'^3 = \frac{\omega'}{c}\cdot \cos(\varphi+\delta), \quad k^0 = \frac{\omega}{c}, \quad k'^0 = \frac{\omega'}{c}.$$

Then equations (13.1) and (13.2) for $\alpha = 3$ can be written as:

$$\omega' = \omega\cdot(cosh\eta_\varphi - r\cdot sin\theta\cdot cos\varphi\cdot sinh\eta_\varphi)$$

$$\omega'\cdot\cos(\varphi+\delta) = \omega\cdot(cos\varphi\cdot cosh\eta_\varphi - \frac{1}{r\cdot sin\theta}\cdot sinh\eta_\varphi)$$

Substituting the first equation into the second one, we get:

$$\cos(\varphi+\delta) = \frac{cos\varphi - \frac{\beta_\varphi}{r\cdot sin\theta}}{1 - r\cdot sin\theta\cdot cos\varphi\cdot\beta_\varphi} \qquad \textbf{(16)}$$

On the radial motion of the wave source or receiver ($g_{00} = 1,\ g_{11} = -1$), we obtain the relativistic Einstein aberration formula [14] from (16).

If $\varphi = \frac{\pi}{2}$, then from (16) we get

$$sin\delta = \frac{\beta_\varphi}{r\cdot sin\theta} \qquad \textbf{(17)}$$

Let's calculate the annual aberration of the stars. We take $r = \frac{\rho}{1au}$ and $\theta = \frac{\pi}{2}$ in formula (17).

1 au = 149 597 870 700 m is an astronomical unit.

On aphelion, the Earth's orbital velocity is $\beta_\varphi = \frac{29.29}{300000}$, and it's $\rho = 1.016$ au from the Sun [15]. On perihelion, the Earth's orbital velocity is $\beta_\varphi = \frac{30.29}{300000}$ and the distance to the Sun is $\rho = 0.98329$ au [15].

ISSN (E): 2181-4570 ResearchBib Impact Factor:6,4 / 2023 SJIF 2024 = 5.073/Volume-2, Issue-10

Calculations using the formula (17) show that the annual aberration angle is equal to:

$\delta_A = 19.80753477''$ – for afelius;

$\delta_P = 21.17978416''$ – for perihelion;

$\bar{\delta} = 20.49365946''$– mean value;

$\delta_{\exp} = 20.49552''$ is the officially accepted annual aberration value [16]. The measurement error ($\Delta = \frac{\delta_{\exp} - \bar{\delta}}{\delta_{\exp}}$) in the calculation of δ is less than $\Delta < 10^{-3}$ %.

We will not consider the case $\alpha = 2$, i.e., motion along the direction of the vector e_θ ($x'^0 = ct'$, $x'^2 = \theta'$, $x^0 = ct$, $x^2 = \theta$, $g_{00} = 1$, $g_{22} = -r^2$, $|\tau_{20}| = r$), since $\alpha = 2$ is a special case of $\alpha = 3$.

Also the case $\alpha = 1$ (radial motion of the source and/or receiver) does not differ from the classical case (Cartesian coordinate system).

6. Hubble's law.

We now find the dependence of the redshift $z = \frac{\omega - \omega'}{\omega'}$ on the distance r between the source and receiver of the wave.

Substituting (15.1) into z, we get

$$z = \frac{sin\theta \cdot \beta_\varphi}{1 - r \cdot sin\theta \cdot \beta_\varphi} \cdot r \qquad (18)$$

To be precise, the "scattering velocity of galaxies" v is by no means equal to, but only proportional to $c \cdot z$ (the product of the speed of light c and the redshift z). Therefore, we

ISSN (E): 2181-4570 ResearchBib Impact Factor:6,4 / 2023 SJIF 2024 = 5.073/Volume-2, Issue-10

multiply formula (18) by $k \cdot c$ and obtain the dependence of the galaxy scattering velocity v on the distance between them r, i.e., Hubble's law [17]:

$$v = k \cdot c \cdot \frac{sin\theta \cdot \beta_\varphi}{1 - r \cdot sin\theta \cdot \beta_\varphi} \cdot r \qquad (19)$$

here $k = 1.28505045 \cdot 10^7 km/c$ is the coefficient of proportionality that is determined by the experiment.

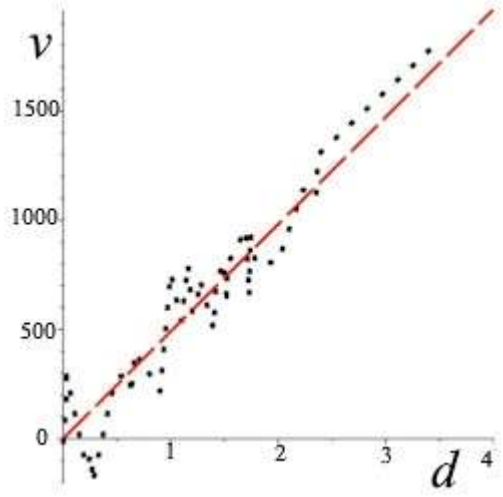

In (19), all variables $(z,\ \beta_\varphi = \frac{v_\varphi}{c}, r)$ are dimensionless, so we accept $r = \frac{d}{R_0}$. $R_0 = 14300\ Mpc$ [18] is the radius of the effective particle horizon, up to which we can see particles created since the Big Bang; d is the distance from the object to the observer, measured in Mpc; Figure 4.

$\beta_\varphi = 24000/300000 = 0.08$ is the linear velocity at the periapsis of S4714's proper orbit [19]. This is the highest velocity in our galaxy (Milky Way).

Then (19) has the form $(sin\theta \approx 1)$:

$$v = \frac{0.08 \cdot k}{R_0 - 0.08 \cdot d} \cdot d \qquad (20)$$

Figure 4 shows the approximation of the data from [20] and [21] by function (20). ■ – data from [20, 21], red dashed line – function (20). We can see that formula (20) agrees well with experiments up to "medium" ($d \sim 500\ Mpc$) distances.

ISSN (E): 2181-4570 ResearchBib Impact Factor:6,4 / 2023 SJIF 2024 = 5.073/Volume-2, Issue-10

If we consider Hubble's law as before, i.e., the dependence $v \sim f(d)$ is linear (Figure 5)

$$v = H(r, \theta, v_\varphi) \cdot d,$$

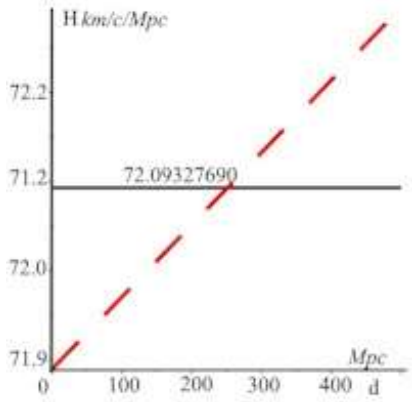

Figure 5.

then we get the Hubble parameter $H(r, \theta, v_\varphi)$:

$$H(d, \theta, v_\varphi) = \frac{sin\theta \cdot \beta_\varphi \cdot k}{1 - sin\theta \cdot \beta_\varphi \cdot d} \quad (21)$$

here $\overline{H} = 72.0932769$ *km/c/Mpc*. $(71.9 < H(d, \theta, v_\varphi) < 72.3)$ is mean value (dark line in Figure 5).

In fact, $H(d, \theta, v_\varphi)$ depends on d, θ and v_φ. Therefore, the Hubble parameter grows weakly with increasing source-receiver distance (Figure 5), even nonlinearly at large distances (dashed red line in Figure 6).

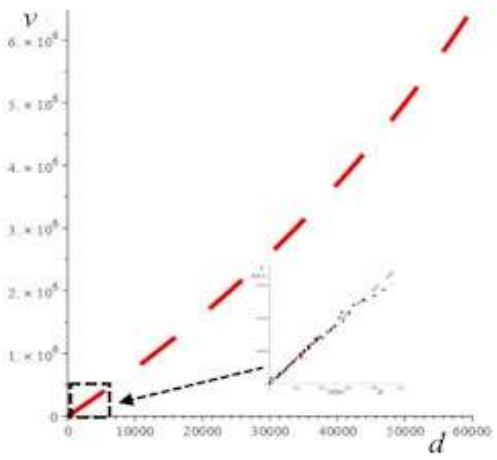

Figure 6.

It would be more correct to take the dependence $z \sim f(d)$ instead of $v \sim f(d)$. Hubble's law was originally derived empirically, also from the assumption that the redshift of the spectrum is due to the radial velocity of objects. In addition, the assumption was that the dependence would be linear. But formula (20) shows that Hubble's law is nonlinear: as the distance between objects increases, the "galaxy expanding velocity", or more precisely, the redshift (Hubble parameter, too), increases even at low velocities and without radial velocity, i.e., without galaxy expand ($v_r = 0$). At large distances, the redshift and Hubble parameter increase with acceleration (Figure 6). The cause of redshift is not only radial motion but also an orbital motion of the source and/or

ISSN (E): 2181-4570 ResearchBib Impact Factor:6,4 / 2023 SJIF 2024 = 5.073/Volume-2, Issue-10

receiver. Simply put, the radial recede of galaxies is not the main reason for redshift. The source and/or receiver's orbital motion is likely the primary cause of the redshift.

Now consider the dependence of redshift z on the zenith angle θ and the distance between objects d: $z \sim f(d, \theta)$.

From (19) we get

$$z = \frac{k \cdot sin\theta \cdot 0.08}{R_0 - sin\theta \cdot 0.08 \cdot d} \cdot d \qquad (22)$$

Figure 7 A shows the relationship (22): $z \sim f(d, \theta)$.

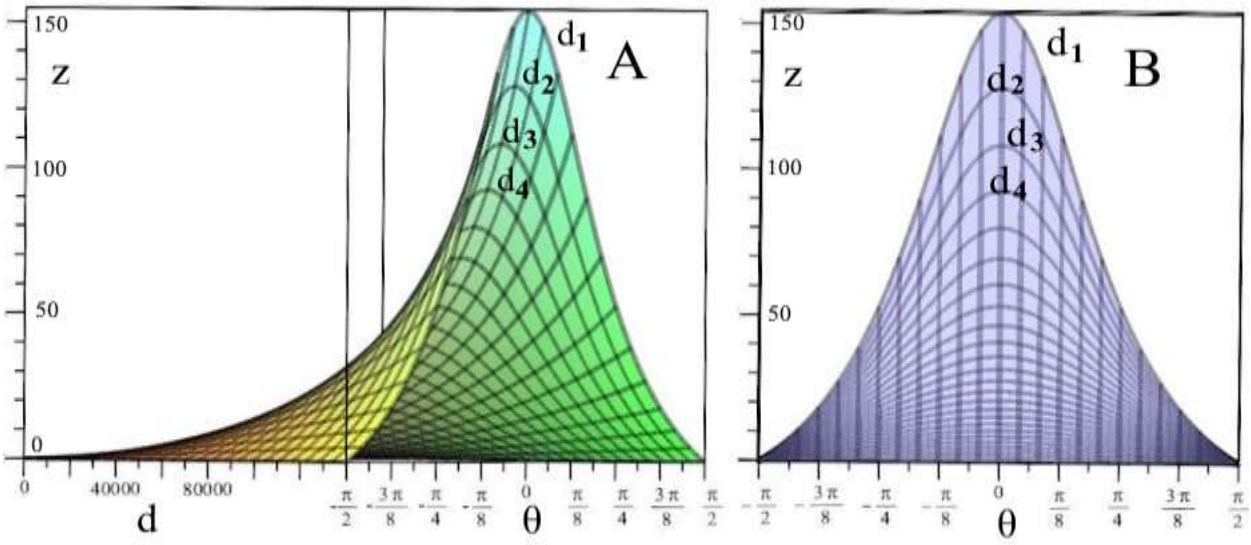

Figure 7.

The two-dimensional plot (Figure 7A) shows that z reaches a maximum at $\theta = \pi/2$ for all values of d ($d_1 > d_2 > d_3 > d_4$). Astronomers often take the angle θ (zero) not from the North Pole [22], but from the ecliptic plane, i.e., from the plane of the Earth's orbit around the Sun. Then we should use $cos\theta$ instead of $sin\theta$ in formula (22). We'll continue that tradition.

ISSN (E): 2181-4570 ResearchBib Impact Factor:6,4 / 2023 SJIF 2024 = 5.073/Volume-2, Issue-10

Figure 7B shows the projection of $f(d,\theta)$ onto the z,θ plane. The graph shows that the closer the angle θ is to the ecliptic ($\theta \to 0$) and the larger the distance d, the larger the redshift z.

We can only observe longitude $0 \le \varphi \le 2\pi$ and latitude $-\pi/2 \le \theta \le \pi/2$ in the sky. We don't see the depth of the sky, i.e., the distance d to the celestial object. We determine it by indirect evidence (brightness, etc.). We calculate the redshift z by formula (22). However, formula (22) depends not on angle φ but on angle θ (Figure 7B).

If the dependence $z \sim f(d,\theta)$ (23) is plotted on a map of the Universe (latitude and longitude), we get the picture as in Figure 8A.

Figure 8B shows a map of the anisotropy of the relic radiation [23] in the K, Ka, Q, V,

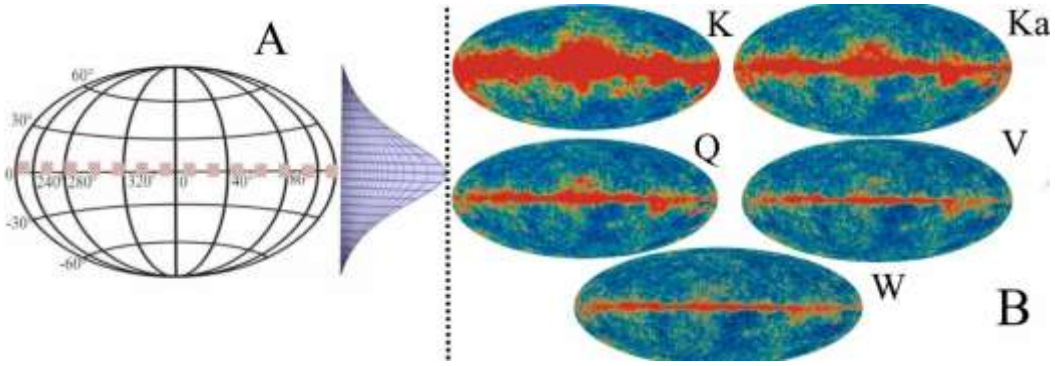

Figure 8

and W bands. A plot of z versus zenith angle θ ($-90^0 \le \theta \le 90^0$ vertically) on the latitude-longitude map is shown on the left (Figure 8A). We see that the z maxima are centered on a narrow band for all d (red shaded band in Figure 8A). In the experiment, the "hot" (red) regions are also located in the center of the ecliptic (Figure 8B). Simply put, the observer (telescope) fixes large ("hot") z 's closer to the ecliptic and small ("cold") z 's farther from the ecliptic. This is similar to how an astronaut from space cannot tell the height of mountain ranges on Earth but only sees stripes where the ridges are.

ISSN (E): 2181-4570 ResearchBib Impact Factor:6,4 / 2023 SJIF 2024 = 5.073/Volume-2, Issue-10

Note again that the width and length of the red shaded band (Figure 8A) depend on z: narrow and short bands correspond to large z, and wide and long bands correspond to small z. This is visually consistent with the data on the right: $K < Ka < Q < V < W$.

The irregularity of the bands in Figure 8B is most likely due to the random distribution of the object velocity and the proximity of the clusters. The "disorderly" arrangement of bright points in cold regions (further from the ecliptic) is probably due to a random distribution of distances d between the source and the receiver (observer).

6. Polarization of the waves

The wave vector changes direction relative to the observer due to the satellite's orbital rotation. The direction of the wave vector changes by an angle δ (aberration angle) due to the rotation of the stars in their orbits and/or the rotation of the Earth around the Sun. The rotation of the source and/or receiver along the orbit is the cause of the change in the direction of the wave vector, causing the change from $\boldsymbol{n}$ to $\boldsymbol{n}'$. This change in the direction of the wave is the cause of the transverse Doppler effect, the aberration, and the polarization of the "refracted" wave.

By analogy with geometrical optics in formula (16), we denote:

$\pi/2 - \varphi = \alpha$ – the angle of incidence of the wave; $\pi/2 - (\varphi + \delta) = \gamma$ – the angle of refraction of the wave;

Considering $\cos(\varphi + \delta) = \cos(\pi/2 - \gamma) = sin\gamma$ and $\cos(\varphi) = \cos(\pi/2 - \alpha) = sin\alpha$ and simplifying from equation (16), we get

$$\frac{sin\alpha}{sin\gamma} = \frac{1 - r \cdot sin\theta \cdot sin\alpha \cdot \beta_\varphi}{1 - \frac{\beta_\varphi}{r \cdot sin\theta \cdot sin\alpha}}$$

ISSN (E): 2181-4570 ResearchBib Impact Factor:6,4 / 2023 SJIF 2024 = 5.073/Volume-2, Issue-10

Let $\theta = \pi/2$. Then

$$\frac{sin\alpha}{sin\gamma} = \frac{1-r\cdot sin\alpha\cdot\beta_\varphi}{1-\frac{\beta_\varphi}{r\cdot sin\alpha}} \qquad (23)$$

By analogy with Snell's law [24], let us introduce the "refractive index" of the vacuum:

$$n = \frac{1-r\cdot sin\alpha\cdot\beta_\varphi}{1-\frac{\beta_\varphi}{r\cdot sin\alpha}} \qquad (24)$$

If $g_{33} = r\cdot sin\alpha = -1$ (rectangular coordinates), then (24) gives $n = 1$– the classical "refractive index" of vacuum. In curvilinear coordinates, the refractive index of vacuum n differs from unity. For example, for an observer on Earth at aphelion $n = 0.9999967655 < 1$, at perihelion $n = 1.000003403 > 1$.

Let the "incident" monochromatic wave $\boldsymbol{n}$ be directed along the unit vector $\boldsymbol{k}$ and the velocity of the wave source be along the unit vector $\boldsymbol{j}$. The direction of the "refracted" wave $\boldsymbol{n}'$ will be $\boldsymbol{k}'$, and the direction of the velocity $\boldsymbol{n}'$ will be $\boldsymbol{j}'$ (Figure 9).

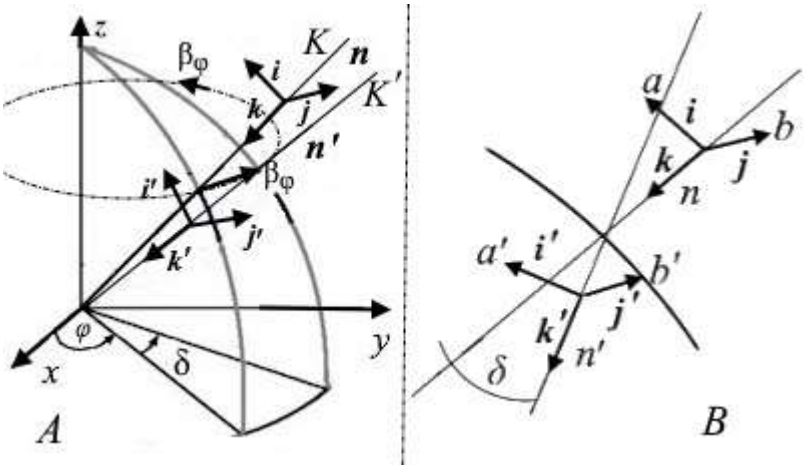

Figure 9

Figure 9A shows the incident wave K and the wave K' (with velocity β_φ on orbit) in a spherical coordinate system. Figure 9B shows the waves K and K' on the incision plane through a vertical plane (the azimuthal angle is φ). Note that $\boldsymbol{j}$ and $\boldsymbol{j}'$ coincide.

We directed $\boldsymbol{n}$ along $\boldsymbol{k}$ freely, at our discretion, and the velocity β_φ **a**long $\boldsymbol{j}$. But the choice of $\boldsymbol{k}', \boldsymbol{j}', \boldsymbol{i}'$ is not free, but rigidly connected with $\boldsymbol{k}, \boldsymbol{j}, \boldsymbol{i}$.

ISSN (E): 2181-4570 ResearchBib Impact Factor:6,4 / 2023 SJIF 2024 = 5.073/Volume-2, Issue-10

Let's consider the electrical components of the "incident" wave:

$$\boldsymbol{E} = \boldsymbol{E}_0 e^{i(\boldsymbol{\hbar r}-\boldsymbol{\omega t})} = \boldsymbol{E}_0 \cos(\boldsymbol{\hbar r} - \boldsymbol{\omega t}) + i\boldsymbol{E}_0 \sin(\boldsymbol{\hbar r} - \boldsymbol{\omega t})$$

$\boldsymbol{\hbar}$ is the wave vector.

Of course, all of the above also applies to the magnetic field.

Let’s introduce vectors:

$$\boldsymbol{a} = \boldsymbol{E}_0 \cos(\boldsymbol{\hbar r} - \boldsymbol{\omega t}) = \boldsymbol{i}a; \qquad \boldsymbol{b} = Re\{i\boldsymbol{E}_0 \sin(\boldsymbol{\hbar r} - \boldsymbol{\omega t})\} = \boldsymbol{j}b;$$

$$\boldsymbol{a}' = \boldsymbol{E}_0' \cos(\boldsymbol{\hbar r} - \boldsymbol{\omega t}) = \boldsymbol{i}a'; \qquad \boldsymbol{b}' = Re\{i\boldsymbol{E}_0' \sin(\boldsymbol{\hbar r} - \boldsymbol{\omega t})\} = \boldsymbol{j}b'.$$

Then

$$\boldsymbol{E} = \boldsymbol{i}a + \boldsymbol{j}b \quad \boldsymbol{E}' = \boldsymbol{i}'a' + \boldsymbol{j}b'$$

Figure 9B clearly shows that the angle between $\boldsymbol{a}$ and $\boldsymbol{a}'$ is equal to δ, as is the angle between $\boldsymbol{i}\hat{}\boldsymbol{i}'$ and between $\boldsymbol{k}\hat{}\boldsymbol{k}'$. The angle between $\boldsymbol{b}$ and $\boldsymbol{b}'$ is zero, as is the angle between $\boldsymbol{j}\hat{}\boldsymbol{j}'$.

The projections of $\boldsymbol{a}'$ onto $\boldsymbol{a}$ and $\boldsymbol{b}'$ onto $\boldsymbol{b}$ are:

$a' = a \cdot cos\delta$ and $b' = b$

The polarization vector is along $\boldsymbol{k}$. Since we have described $\boldsymbol{n}$ in the right-handed coordinate system (right-handed vector triad), $\boldsymbol{n}'$ will also be right-handed polarized.

Let's find the polarization vector P (let $a = b$):

$$P = \frac{E_j^2 - E_i^2}{E_j^2 + E_i^2} = \frac{b^2 - a^2 cos^2\delta}{b^2 + a^2 cos^2\delta}$$

ISSN (E): 2181-4570 ResearchBib Impact Factor:6,4 / 2023 SJIF 2024 = 5.073/Volume-2, Issue-10

Incident wave ($\boldsymbol{n}$) is natural, not polarized. For natural light, where waves of different polarizations are equally mixed and all directions are equal. Assuming that the polarized wave $\boldsymbol{n}'$ (after "refraction") is half the natural wave, we get:

$$P = \frac{1}{2} \cdot \frac{1-cos^2\delta}{1+cos^2\delta} \qquad (25)$$

From formula (25), we can find the degree of polarization for annual aberration.

Substituting (17) into (25) and simplifying, we get:

$$P = \frac{1}{2} \cdot \frac{sin^2\delta}{2-sin^2\delta} = \frac{0.5}{2 \cdot sin^{-2}\delta - 1} \quad \text{or}$$

$$P = \frac{0.5}{2 \cdot \beta_\varphi^{-2} \cdot r^2 \cdot cos^2\theta - 1} \qquad (26)$$

At aphelion ($\beta_\varphi = \frac{29.29}{300000}$, $r = 1.0167\ au$, $\theta = 0$) – $P_a = 2.31 \cdot 10^{-9}$.

At perihelion ($\beta_\varphi = 30.29/300000$, $r = 0{,}98329\ au$, $\theta = 0$) – $P_p = 2.64 \cdot 10^{-9}$.

We took the zenith angle from the ecliptic, following the astronomers: ($sin\theta \to cos\theta$). Of course, the effects are very weak: $P_a = 2.31 \cdot 10^{-9}$ and $P_p = 2.64 \cdot 10^{-9}$.

In general, the degree of polarization (26) depends on the distance between the source and receiver and the zenith angle (elevation angle).

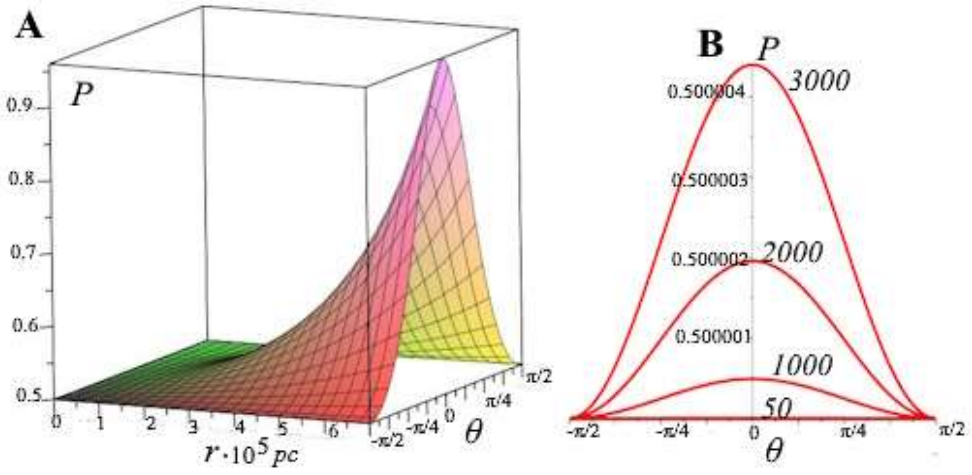

This dependency is illustrated in Figure 10: $\beta_\varphi = 10^{-4}$ – Earth's average orbital

ISSN (E): 2181-4570 ResearchBib Impact Factor:6,4 / 2023 SJIF 2024 = 5.073/Volume-2, Issue-10

velocity; Figure 10. r – distance from observer (on Earth) to wave source; $R_0 = 14300 \cdot 10^6\ pc$ [18].

The dependences of $P \sim f(\theta)$ at 50, 1000, 2000, and 3000 parsecs are shown in Figure 10B. Graph 10B is an incision of the 3-dimensional graph 10A by the plane θ: $P \sim f(r, \theta)$. It is obvious that for large r and $\theta \sim 0$, the degree of polarization P is maximum.

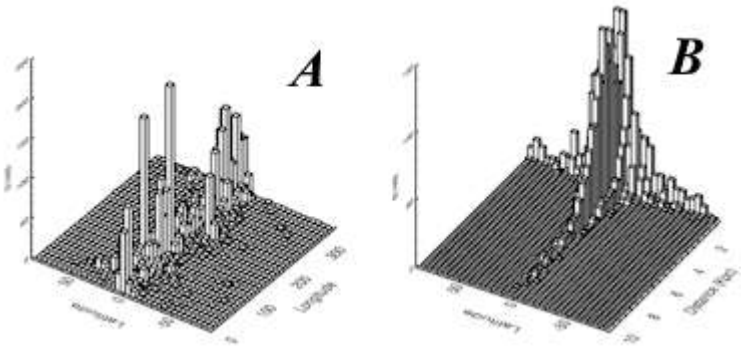

Figure 11

Figure 11 shows plots of experimental data on measurements of the degree of polarization of stars [25]. Graph 10A does not conflict with Graph 11B, which is the experiment. Diagram 11A doesn't contradict the Graph 10B, if the latter is placed on the θ, φ plane.

It is obvious that here, as in the case of the redshift (Figure 8), we also see a stripe close to the ecliptic ($\theta \sim 0$) (Figure 12).

Figure 12 shows starlight polarization vectors in galactic coordinates for 5513 stars. [52] for a local cloud (upper) and for an average polarization vector over many clouds (lower). . (нижняя). Our calculations for measuring the degree of polarization do not include statistical hypothesis testing (due to the small sample). Nevertheless, both graphs (Figures 11 and 12) visually demonstrate the correctness of our

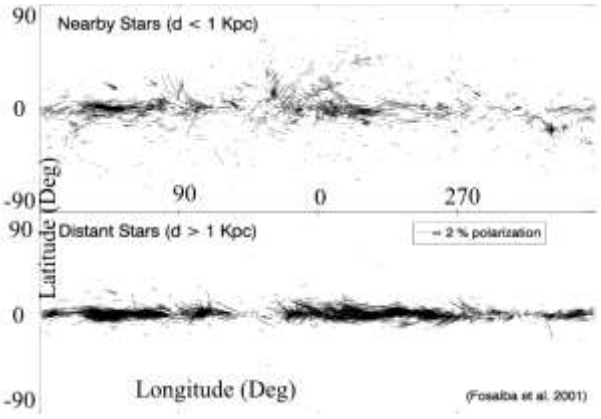

Figure 12.

ISSN (E): 2181-4570 ResearchBib Impact Factor:6,4 / 2023 SJIF 2024 = 5.073/Volume-2, Issue-10

assumption about the dependence of the degree of polarization on distance and polar angle: the greater the distance between the source and receiver of the wave and the closer the elevation angle to the ecliptic ($\theta \sim 0$), the greater the degree of polarization. In other words, large redshifts z and maximum degrees of polarization P are concentrated near the ecliptic plane.

Discussions and Conclusions

1. Generalized biquaternions are a convenient and universal mathematical tool for describing many physical processes, in particular the Lorentz transformation and its consequences (the Doppler effect, aberration, and polarization of light) in curvilinear coordinates.

2. The radial running away of galaxies (longitudinal Doppler effect) is not a necessary and single cause of red shift. The rotation of the source and/or receiver of the wave along the orbit is, perhaps, the main cause of the red shift of the spectrum of stars. In other words, in a stationary universe, there is also a redshift of the spectrum of stars.

3. The rotation of the source and/or receiver of the wave along the orbit, which is (mathematically) the Lorentz transformation in curvilinear coordinates, is the cause of both the redshift and the aberration and polarization of the wave and is also gravitational lensing, i.e., the "refractive index of space-vacuum" is not equal to the unit ($n \neq 1$).

4. The greater the distance between the source and receiver of the wave, the greater the redshift and degree of polarization of the wave, and they are concentrated in a narrow band near the plane of the ecliptic ($\theta \sim 0$).

Acknowledgements

ISSN (E): 2181-4570 ResearchBib Impact Factor:6,4 / 2023 SJIF 2024 = 5.073/Volume-2, Issue-10

It should be noted that without the experimental data [20], [21], [23], and [25], it is unlikely that I would have been able to verify the theoretical assumptions presented in the article. I would like to express my gratitude to my ally, my wife Lyuba Gomazkova, for correcting and formatting the Russian version of the text and formulas, for creating a cozy and comfortable working environment, and, above all, for her angelic patience. And in general, I would like to express my gratitude to everyone who contributed to the emergence of this work.

References

1. Transverse Doppler Effect and Special Relativity. E. Falkner. The General Science Journal. https://www.gsjournal.net/Science-Journals/Research%20Papers-Relativity%20Theory/Download/7621

2.The global positioning system, relativity, and extraterrestrial navigation Neil Ashby and Robert A. Nelson 2008. https://tf.nist.gov/general/pdf/2444.pdf

4. Pain, Reynald; Astier, Pierre (2012). "Observational evidence of the accelerated expansion of the Universe". *Comptes Rendus Physique*. **13** (6): 521–538. arXiv:1204.5493 pp. 13-16. .

5. Jacques Colin, Roya Mohayaee, Mohamed Rameez and Subir Sarkar (Nov 2019). "Evidence for anisotropy of cosmic acceleration⋆". *Astronomy & Astrophysics*. 631: L13. arXiv:1808.04597.

6. Freedman, W. L.; Madore, B. F. (2010). The Hubble Constant. *Annual Review of Astronomy and Astrophysics*. 48: 673–710. arXiv:1004.1856.

7. Sangwine, Stephen J.; Ell, Todd A.; Le Bihan, Nicolas (2010), "Fundamental representations and algebraic properties of biquaternions or complexified quaternions", *Advances in Applied Clifford Algebras*, 21 (3): 1–30, *arXiv*:*1001.0240*,

ISSN (E): 2181-4570 ResearchBib Impact Factor:6,4 / 2023 SJIF 2024 = 5.073/Volume-2, Issue-10

8. The rules of 4-dimensional perspective: How to implement Lorentz transformations in relativistic visualization. Andrew J. S. Hamilton. arXiv:2111.09307v1 [gr-qc] 16 Nov 2021

9. Babaev A. Kh., Biquaternions, rotations, and spinors in the generalized Clifford algebra (in Russian). Sci-article.ru. № 45 (May) 2017. pp. 296 - 304, https://sci-article.ru/number/05_2017.pdf

10. Chris J. L. Doran. Geometric Algebra and its Application to Mathematical Physics. Sidney Sussex College. A dissertation submitted for the degree of Doctor of Philosophy in the University of Cambridge. February 1994, pages 4-6.

11. Gaston Casanova. L'Algebre Vectorielle. Press Universitaires de France. p. 10, 19. https://books.google.ru/books?id=Es__EAAAQBAJ&pg=PA2&hl=ru&source=gbs_toc_r&cad=2#v=onepage&q&f=false

12. Babaev A. Kh. Alternative formalism based on Clifford algebra (in Russian), SCI-ARTICLE.RU. №40 (December) 2016, pp. 34 – 42, https://sci-article.ru/number/12_2016.pdf

13. Landau L. D., Lifshitz E. M., The Classical Theory of Fields, Course of Theoretical Physics, vol. 2, pp. 123 – 127.

14. Albert Einstein (1905) "*Zur Elektrodynamik bewegter Körper*", *Annalen der Physik* 17: 891; English translation

15. https://en.wikipedia.org/wiki/Earth%27s_orbit

16. https://en.wikipedia.org/wiki/Astronomical_constant

17. Dan Scolnic, Lucas M. Macri, Wenlong Yuan, Stefano Casertano, Adam G. Riess. Large Magellanic Cloud Cepheid Standards Provide a 1% Foundation for the Determination of the Hubble Constant and Stronger Evidence for Physics Beyond LambdaCDM – 2019-03-18. arXiv:1903.07603.

18. Gott III, J. Richard; Mario Jurić; David Schlegel; Fiona Hoyle; et al. (2005). "A Map of the Universe" (PDF). *The Astrophysical Journal*. **624** (2): 463–484. arXiv:astro-ph/0310571.

ISSN (E): 2181-4570 ResearchBib Impact Factor:6,4 / 2023 SJIF 2024 = 5.073/Volume-2, Issue-10

19. Florian Peißker, Andreas Eckart, Michal Zajaček, Basel Ali, Marzieh Parsa. S62 and S4711: Indications of a population of faint fast moving stars inside the S2 orbit -- S4711 on a 7.6 year orbit around Sgr~A* // The Astrophysical Journal. — 2020-08-11. — v. 899, Edit. 1. — S. 50. — ISSN 1538-4357

20. Hubble, E. (1929). "A relation between distance and radial velocity among extra-galactic nebulae". *Proceedings of the National Academy of Sciences*. 15 (3): 168–173.

21. W. L. Freedman, B. F. Madore, B. K. Gibson, L. Ferrarese, D. D. Kelson, S. Sakai, J. R. Mould, R. C. Kennicutt Jr., H. C. Ford, J. A. Graham and others, Hubble, E. (1929). "A relation between distance and radial velocity among extra-galactic nebulae". *Proceedings of the National Academy of Sciences*. 15 (3): 168–173. Final Results from the Hubble Space Telescope Key Project to Measure the Hubble Constant, https://arxiv.org/abs/astro-ph/0012376

22. https://en.wikipedia.org/wiki/Ecliptic

23. First Year Wilkinson Microwave Anisotropy Probe (WMAP) Observations: Preliminary Maps and Basic Results, C.L. Bennett, et al., 2003ApJS..148....1B, reprint / preprint (4.4 Mb) / individual figures / ADS / astro-ph, https://lambda.gsfc.nasa.gov/product/wmap/pub_papers/firstyear/basic/wmap_cb1_images.html

24. https://en.wikipedia.org/wiki/Snell%27s_law

25. Pablo Fosalba (IAP), Alex Lazarian (Wisconsin), Simon Prunet (CITA), Jan A. Tauber (ESA-ESTEC). Dust Polarization From Starlight Data.https://arxiv.org/abs/astro-ph/0111253

Dear Prof. Steven K. Lamoreaux and Prof. Ryan Davies.

1. I am not affiliated with any institute at the moment. I am a freelancer. I worked at the Institute of Nuclear Physics, National University (Tashkent, Uzbekistan). Then I worked at the Novosibirsk State Technical University (RF) by invitation.

2. Although I am ethnically Uzbek, I live in the RF, in Novosibirsk, since my family and

ISSN (E): 2181-4570 ResearchBib Impact Factor:6,4 / 2023 SJIF 2024 = 5.073/Volume-2, Issue-10

grandchildren live here.

I am writing this because

1) Due to the aggression of the RF against Ukraine, there are a lot of restrictions for those from Russia;

2) It is impossible to transfer money from Russia anywhere, for example, for processing and preparing an article.

3. I finished and translated this article into English literally today and therefore have not sent it anywhere for publication yet.

4. Since I am a freelancer and not affiliated with anyone, I am the only author of the article.

Best Regards Babaev A.Kh.